

# Helicon plasma with additional immersed antenna

A Aanesland<sup>1,2</sup>, C Charles<sup>1,3</sup>, R W Boswell<sup>1</sup> and Å Fredriksen<sup>2</sup>

<sup>1</sup> Plasma Research Laboratory, Research School of Physical Sciences and Engineering, Australian National University, ACT 0200, Australia

<sup>2</sup> Physics Department, University of Tromsø, N-9037 Tromsø, Norway

E-mail: ane@phys.uit.no

Received 23 June 2003

Published 14 April 2004

Online at [stacks.iop.org/JPhysD/37/1334](http://stacks.iop.org/JPhysD/37/1334)

DOI: 10.1088/0022-3727/37/9/006

## Abstract

A 'primary' RF power (H-power) at 13.56 MHz is coupled to a plasma source excited by an external double saddle field Helicon antenna. A 'secondary' RF power (S-power), also at 13.56 MHz but with variable phase, is additionally coupled by inserting a second antenna in contact with the plasma through one end of the source. The immersed antenna can be grounded or floating, allowing a self-bias to form in the latter case. Changes in the plasma density and electron temperature are measured in both cases with varying power on the immersed antenna. The plasma potential increases dramatically with S-power in the grounded case, and is found to be similar in size to the sum of the plasma potential and the self-bias formed in the floating case for all powers. Hence, the sheath between the immersed antenna and the plasma is shown to be equal in both the grounded and floating cases. Although the power efficiency does not vary significantly as a function of the S-power, it is consistently lower for the grounded case possibly as a result of a dc current to ground. The plasma parameters are drastically changed as the phase between the two antennae are varied (floating case), and a sinusoidal function was fitted to the plasma parameters as a function of the phase shift. The calculated power loss to the antenna indicates that the power efficiency of the immersed antenna, as the phase is changed, is altered from 80% to 10%.

## 1. Introduction

In general, high density, low pressure plasma sources are excited by rf fields generated by antennae exterior to and physically separated from the actual plasma. Usually, the separation medium is simply a glass vacuum vessel and the plasma may be excited by capacitive coupling of the voltage difference across the antenna or by inductive coupling of the electric fields induced by currents in the antenna. A so-called 'inductively coupled' plasma will have both phenomena operating, although the inductive electric field is generally dominant. As it is generally difficult (and often undesirable) to eliminate capacitive coupling, the glass dielectric vacuum vessel in contact with the plasma next to the antenna will charge up negatively [1] to form a bias voltage. This will accelerate

ions locally into the glass and produce secondary electrons that will subsequently be accelerated by the same bias field into the plasma bulk, thereby providing an extra source of ionization. As the area of the antenna is usually much smaller than the area of the plasma source, these areas of negative bias are quite small and, in general, can be neglected compared to the inductive coupling. Hence, the majority of inductively (and microwave) coupled plasmas have a low plasma potential of a few tens of volts and floating potentials close to 0 V.

For processing applications, a rf biased substrate can be introduced into the plasma produced by the inductive coupling, allowing the ion energies impinging upon the substrate surface to be controlled independently of the current to the substrate, which is determined by the rf power to the inductive coupling [2]. This effect is made use of in some industrial, capacitively coupled plasmas to etch insulators using ion bombardment or reactive ion etching. The powered electrode in these systems is

<sup>3</sup> Also at: Département Sciences Pour l'Ingénieur Centre National de la Recherche Scientifique, France.

in contact with the plasma but in the matching network there is a tune capacitor that plays the role of a DC block, allowing the electrode to develop a negative self-bias with current flowing only during the charge up stage of the capacitor (some tens of  $\mu\text{s}$ ). This phenomenon is essentially the same as that described by Butler and Kino [1] with the glass vacuum vessel playing the role of the blocking capacitor.

Antennae are also usually situated inside the vacuum vessel in plasma fusion experiments and are often in contact with the plasma. In particular, in the H1 Heliac experiment at the Australian National University [3], the rf antenna is shaped like a loop in the plane of the last closed flux surface (LCFS) and is in contact with the plasma. One end of the loop is grounded, allowing direct currents to flow from the plasma. For typical conditions of 70 kW of rf at 7 MHz, the plasma potential at the LCFS is over 100 V while at the plasma centre it is about 0 V. A current of about 90 A of electrons has been measured going to earth, which probably maintains the edge plasma potential at +100 V. Similar effects have been noted in experiments on plasma immersion ion implantation (PI3) where the rf antenna is generally inside a large metallic vacuum chamber [4, 5].

If the plasma source and biased substrate frequencies are significantly different from each other there is little or no interaction between the two frequencies [6]. However, the substrate is sometimes biased with the same rf frequency as the source, and to avoid beating, the phase difference between the two rf voltages (to the plasma source and the substrate) is controlled electronically. Thomas and Singh [7] showed that the phase of the rf voltage applied to the electrodes in a balanced triode etching system had a profound effect on the resulting plasma and etch rate. A rf glow discharge sputtering model together with experiments showed that the phase delay between a cathode and a substrate affect both the electron and ion energies, the peak-to-peak voltages on the

electrodes and the rf input power on the substrate [8]. It has also been reported that phase regulation in inductively coupled and unbalanced magnetron rf biased sputtering systems can change the self-bias at substrate samples as well as the ion energy distribution [9, 10].

In this work, we measure the influence on the plasma parameters of the rf power supplying a copper antenna (biased substrate) immersed into a plasma generated by an external helicon antenna (source). The immersed antenna can be either grounded or floating. The influence on the plasma parameters of the phase shift between the rf supplying the external helicon antenna and the immersed copper antenna is investigated.

## 2. Experimental set-up

The helicon system used for the experiments reported here has been described previously [11, 12] but has been modified by the insertion of a second copper antenna which is immersed in, and in contact with, the plasma [13]. A sketch of the system is shown in figure 1. Briefly, the plasma is excited by a 20 cm long double saddle type helicon antenna surrounding and outside the 15 cm diameter glass source tube. A 6 cm long bare copper antenna is inserted through the aluminium source end plate and extends 8 cm into the plasma. The helicon and small immersed antennae will be referred to as the H-antenna and S-antenna, respectively. Both antennae are fed by rf power at 13.56 MHz with separate matching networks and rf generators. The power on the S-antenna is 10–100 W and capacitively and/or inductively coupled to the plasma. The power on the H-antenna is 150 W, which is generally low compared to common helicon systems, and the power is mainly inductively coupled to the plasma [13, 14]. However, for a plasma density of  $10^{11} \text{ cm}^{-3}$  in a magnetic field of 100 G, the helicon wavelength would be around 50 cm, so helicon fields would be present throughout the system, although previous

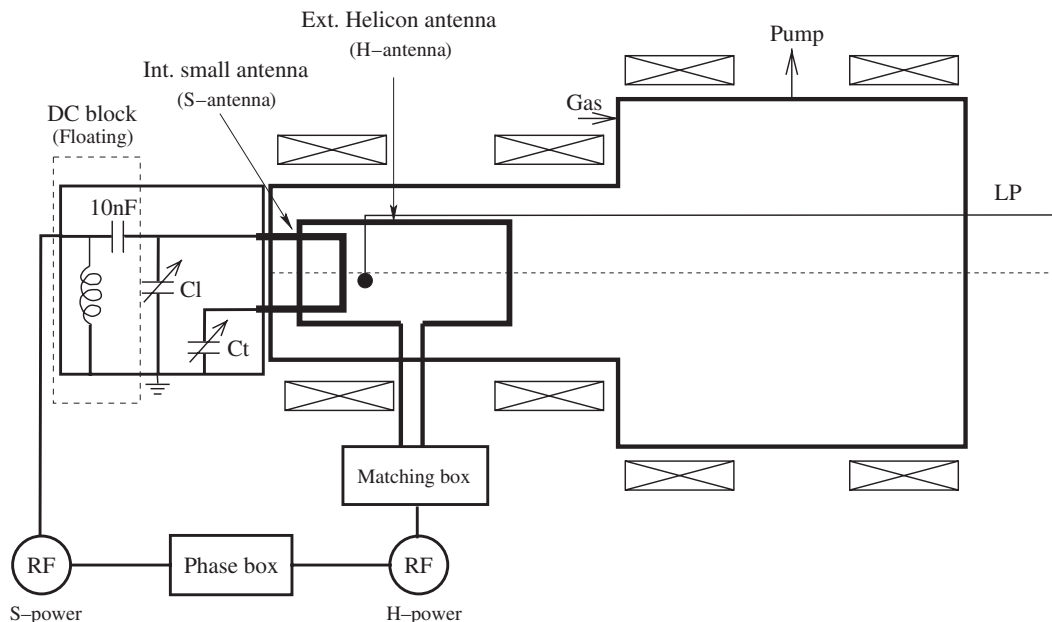


**Figure 1.** A schematic diagram of the experimental set-up 'Chi-Kung'. For better clarity SWR meters inserted between the rf generators and the matching circuits are not shown in the figure.

experience with this system has shown that it is unlikely that the helicon enters into the ionization process at this low power.

The S-antenna can be directly connected to ground, allowing a direct current to flow, or it can be isolated from ground by a blocking capacitor as shown in figure 1. In the latter case, the blocking capacitor can charge up and impose a negative self-bias on the S-antenna. The differences between these two situations will be discussed in this paper.

The phase difference between the two antennae is electronically controlled and can be changed from 0 (in phase) to  $\pm 180^\circ$  out of phase, by a common phase control unit connected between the two rf generators. For convenience, the rf signal to the helicon antenna is maintained at a fixed phase, while the phase of the rf signal from the generator to the immersed antenna is varied with respect to this fixed phase. The phase difference between the two antennae is calibrated by measuring the phase of the input voltages with a directional coupler between the generators and the matching networks.

The argon feed gas is introduced into the diffusion chamber, and the turbomolecular/rotary pumping system is connected to the sidewall of the chamber. The base pressure is a few  $10^{-6}$  Torr, the pressure being measured with an ion gauge and a Baratron gauge. Two solenoids situated around the source are used to create a dc magnetic field. A pressure of 4 mTorr and a magnetic field of 100 G in the source, decreasing to a few Gauss in the diffusion region, were used.

A low pass filter connected to the immersed antenna inside the matching box was used to measure the antenna self-bias ( $V_{sb}$ ). The peak-to-peak value of the rf current ( $I_{pp}$ ) in the matching box was measured using a rf current coil (Rogowsky coil) around the high voltage side of the immersed antenna.

A Langmuir probe (LP) was inserted 1 cm from the S-antenna, in the horizontal plane of the antenna, to obtain the plasma density ( $n_i$ ), the electron temperature ( $T_e$ ), the plasma ( $V_p$ ) and floating potentials ( $V_f$ ). As the sheath thickness in front of the S-antenna is typically 0.02 cm the LP results taken 1 cm away from the antenna will reflect the bulk plasma parameters. The Langmuir characteristics

are obtained using a Labview acquisition system, where the probe voltage,  $V_{pr}$ , is swept from +40 to  $-30$  V with an increment of 0.7 V (100 steps), and the voltage is kept at  $-30$  V between the sweeps. The ions are unmagnetized at a maximum magnetic field of  $< 100$  G, hence a non-magnetized theory to obtain the plasma density from the ion saturation current can be used [15]. The plasma potential is found by the maximum of the first derivative together with the zero crossing of the second derivative of the characteristics. RF plasma potential fluctuations can alter the characteristics measured by a Langmuir probe, but in our case the second derivative of the characteristic, typically has a maximum and minimum separated by less than  $2kT_e$ , and the amplitude of the floating potential fluctuations is less than  $kT_e$ , which indicates that the effect of RF on the LP measurements are negligible [16].  $T_e$  is found from the half-logarithmic plot of the electron current, and the straight line was extended over two or more decades. An experimental curve is shown in figure 2 where the linearity of the plot is quite clear and strongly suggests that rf interference is very small. The errors were deduced from repeated analysis of the same IV characteristics, and were found to be of the order of  $\Delta V_p = 0.5$  V,  $\Delta V_f = 0.7$  V,  $\Delta T_e = 0.5$  eV. The results for  $n_i$  are correct to within 20%, including the errors in both the ion saturation current and the electron temperature. The LP acquisition system and analysis are described in more detail in previous studies [13, 17].

### 3. Results and discussion

#### 3.1. Grounded immersed antenna

The initial results were obtained with the S-antenna grounded. The power on the Helicon antenna (H-power) was 150 W and the two antennae were in phase ( $0^\circ$  phase shift). Figures 3 and 4 show the response of  $V_p$ ,  $V_f$ ,  $T_e$  and  $n_i$  to increasing power on the S-antenna (S-power). When the S-power increases from 10 to 50 W the plasma potential, floating potential and electron temperature increase from 30 V to 80 V, 20 V to 50 V and

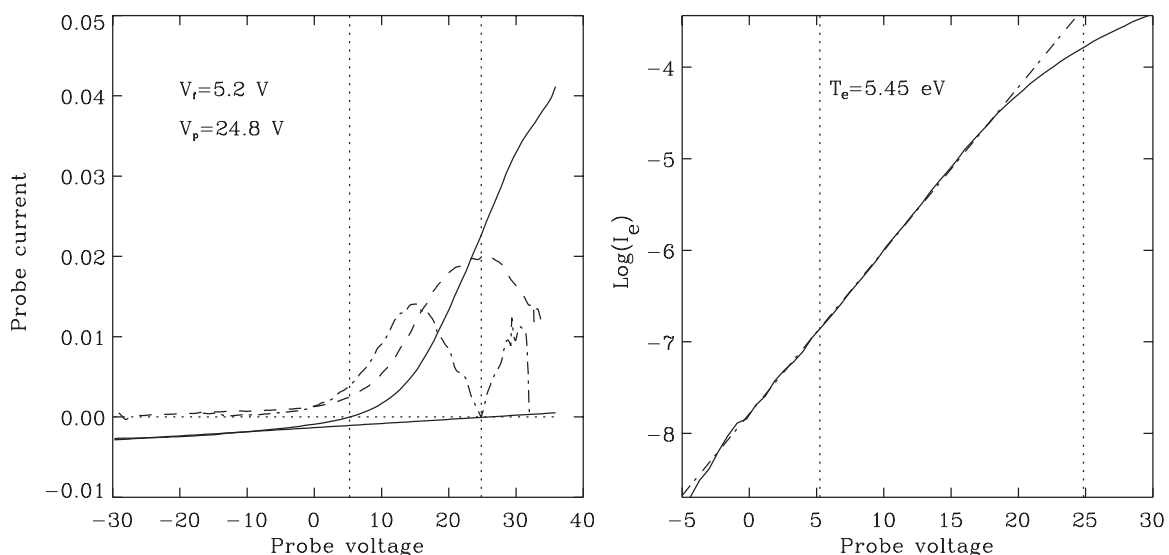


**Figure 2.** (Left) The LP characteristic, the 1st derivative and the absolute values of the 2nd derivative. (Right) The half-logarithmic plot of the electron current. The dotted lines are the floating and plasma potentials. This data is obtained with the S-antenna floating at 90 W.

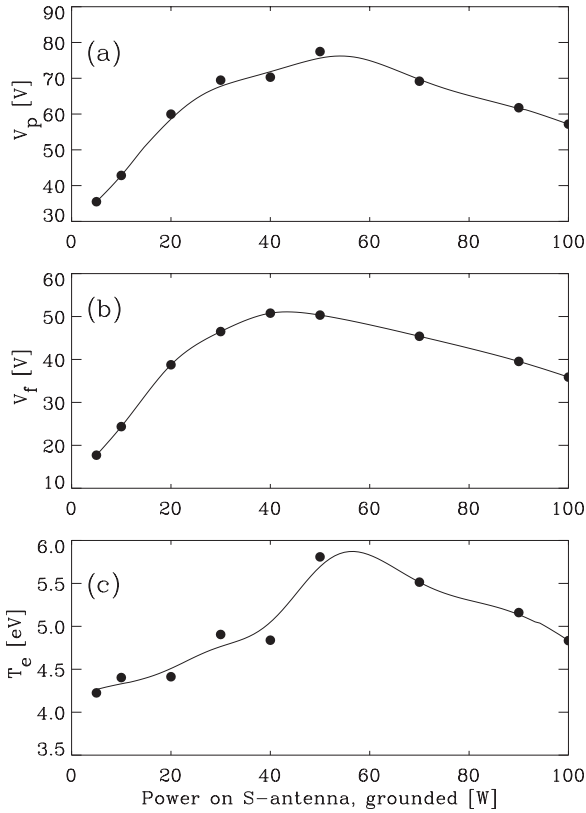


**Figure 3.** (a) Plasma potential  $V_p$ , (b) floating potential  $V_f$  and (c) electron temperature  $T_e$  as a function of S-power. The results are obtained with the LP 1 cm away from the grounded immersed S-antenna. H-power and argon pressure are 150 W and 4 mTorr, respectively. The phase shift between the H- and S-antennae is zero.

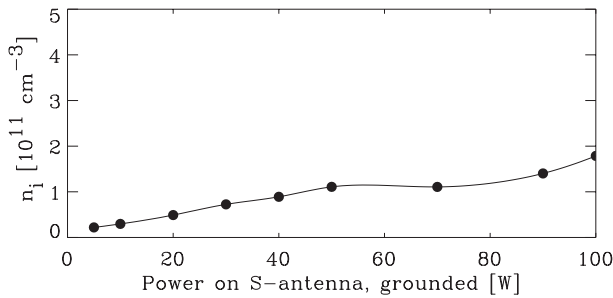


**Figure 4.** Plasma density  $n_i$  as a function of S-power, for the same conditions as in Figure 3.

4.2 eV to 5.7 eV, respectively, and then slightly decrease for powers above 50 W. We note here that the plasma potential, the floating potential, and the electron temperature trace each other well. The plasma density increases linearly with S-power by one order of magnitude from about  $2 \times 10^{10} \text{ cm}^{-3}$  to  $1.8 \times 10^{11} \text{ cm}^{-3}$ . These measurements were made quite close to the S-antenna (1 cm), and for the working pressure of 4 mTorr, the plasma density decreased axially away from the S-antenna. The most interesting phenomenon is the increase in the plasma and floating potentials as the S-power is increased. At the higher powers, many small pinpoint discharges could be seen in the diffusion chamber. This phenomenon had been previously seen in our laboratory when there was no blocking capacitor in a capacitively driven discharge. To set the background for this

phenomenon, it is worthwhile to recall that in an asymmetric discharge (such as we have here), the voltage division between the sheath on the powered electrode (here the S-antenna) and the sheath on the ground electrode (here the diffusion chamber) is given by

$$Z = Z_1 + Z_2 = \frac{1}{C_1 \omega} + \frac{1}{C_2 \omega}, \quad (1)$$

where  $C_1$  and  $C_2$  are the capacitances of the two sheaths. The capacitance is given by  $\epsilon_0 A/d$ , where  $A$  is the electrode area and  $d$  is the sheath thickness in front of the electrodes. Since the area of the grounded electrode is much larger than that of the powered S-electrode, and the thickness of the sheath on the grounded electrode is much less than that of the powered S-electrode, the capacitance of the sheath on the S-antenna is orders of magnitudes smaller than that of the earthed electrode. Hence, its impedance will dominate that of the earthed sheath and most of the rf voltage on the S-electrode will appear across the S-electrode to the plasma sheath. As the plasma is a good conductor, this high rf voltage will lead to a high dc voltage that will appear everywhere in the plasma, in particular, in the diffusion chamber. As the impedance of the earthed sheath is very small, it supports only a small rf potential difference but the plasma enforces a much higher dc potential difference. It would appear that, under these circumstances, the pinpoint discharges are observed. The detailed physics of their appearance and evolution is not yet known.

### 3.2. Dc isolated immersed antenna

A second set of experiments was carried out with the same experimental conditions as above, but with the S-antenna isolated from ground by a 10 nF blocking capacitor. Figures 5 and 6 show the response of  $V_p$ ,  $V_f$ ,  $T_e$ ,  $n_i$ , and  $V_{sb}$  to increasing power on the S-antenna (S-power). In this case, the plasma and floating potentials remain relatively constant. When the S-power increased from 5 to 100 W, the increase of  $T_e$  and  $n_i$  by 2 eV and a factor of 10, respectively, is similar to the grounded S-antenna case. However, the density in the floating case remains one to three times higher than that measured for the grounded case.

Below 30 W, the self-bias shows a linear dependence on the S-power. A linear relationship between a substrate self-bias and RF power from 0 to 30 W together with an unchanged plasma potential has been obtained previously in a dual RF excitation plasma [18]. A self-consistent, three moment, fluid model of a dually driven rf plasma also confirms this behavior [19]. It was shown by both authors that this dependence is independent of substrate frequency. The relationship is explained by Goto *et al* [18] as follows. The substrate power (S-power) is given by

$$P_S = I_{dc} \cdot V_{dc} \quad (2)$$

and roughly

$$I_{dc} \propto n_i \cdot \sqrt{T_e}. \quad (3)$$

Because of the small powers, the substrate or antenna does not perturb the plasma and hence  $n_i$  and  $T_e$  are unchanged (as confirmed by the results in figures 2 and 3 for powers  $\leq 30$  W). The combination of the above equations shows that

$$V_{dc} \propto V_{sb} \propto P_{AS}. \quad (4)$$

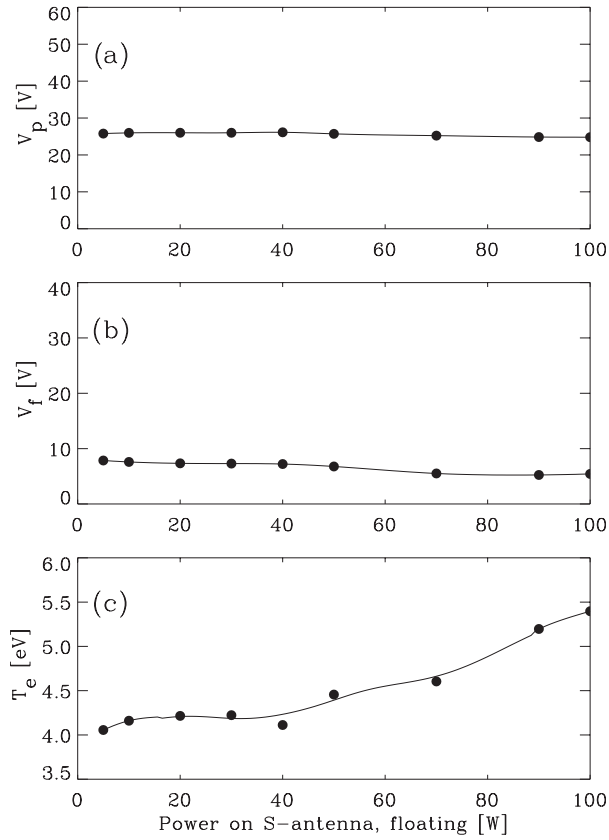


**Figure 5.** (a) Plasma potential  $V_p$ , (b) floating potential  $V_f$  and (c) electron temperature  $T_e$  as a function of S-power. The results are obtained with the LP 1 cm away from the floating immersed S-antenna. The H-power and argon pressure are 150 W and 4 mTorr, respectively. The phase shift between the H- and S-antennae is zero.

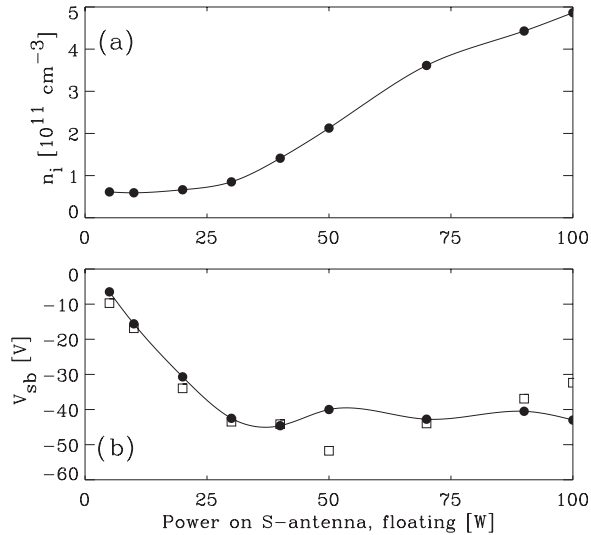


**Figure 6.** (a) Plasma density  $n_i$  and (b) self-bias  $V_{sb}$  as a function of S-power, for the same conditions as in figure 5. The values for  $V_p(\text{float}) - V_p(\text{ground})$  are shown as open squares.

Goto *et al* concluded that if the substrate power (S-power) becomes comparable to the ‘plasma generating power’ (H-power) the above argument is incorrect. To our knowledge, there have been no investigations previously on dually driven rf plasma sources showing the effect on the self-bias when the

rf substrate power and the plasma generating power become commensurate. However, as can be seen from our results, above 30 W the S-antenna indeed affects the bulk plasma as both the plasma density and temperature increase, and  $I_{dc}$  is no longer constant. We observe that above 30 W,  $V_{sb}$  is constant and  $P_{AS} \propto I_{dc}$ . Hence, as soon as the S-power is high enough the power goes to increasing the plasma density and electron temperature and the self-bias is kept constant. The constant  $V_{sb}$  might be due to a capacitive-to-inductive transition at this power for the floating case. When the antenna is grounded, a direct current can flow from the plasma through the match box to ground and results in an additional Ohmic loss term that can reduce the plasma density.

The self-bias ( $V_{sb}$ ) on the S-antenna is almost exactly a mirror image of the plasma potential for the grounded S-antenna case. The plasma potential,  $V_p$  (grounded), in the grounded case is related to the one in the floating case,  $V_p(\text{float})$  by

$$V_p(\text{ground}) = V_p(\text{float}) - V_{sb}. \quad (5)$$

The values of  $[V_p(\text{float}) - V_p(\text{ground})]$  versus S-power, shown by open squares in figure 6(b), are very similar to the values of  $V_{sb}$ . A possible way of viewing this phenomenon is by using the impedance division argument between a small powered antenna and a large earth, presented previously. In the asymmetric capacitive discharge with a blocking capacitor, a self-bias develops on the small powered electrode with a magnitude close to that of the rf voltage applied. Whilst the capacitor is charging, a current flows with electrons going to the capacitor and ions being lost from the discharge to the earthed walls. It is commonly accepted that this occurs because of the differences in impedances between the sheath capacitances on the powered and earthed electrodes. If the antenna is earthed, the rf on the antenna will force a dc voltage component to appear on the plasma in much the same way as in a symmetric capacitively coupled discharge. This dc potential would play the role of a plasma potential which we measure. It would appear from our results, that for the present experimental configuration, the potential difference between the antenna and the plasma must be maintained, whether the antenna be grounded or floating. We do not have a detailed explanation but apparently this phenomenon can give rise to dangerous discharges separated by some distance from the powered (small immersed) antenna. Similar results of large plasma potentials have been reported on previously in PI3 systems, with internal dc grounded antennae [4], and in the H1 Helic experiment also using a dc grounded antenna [3]. However, the above relation has not been previously reported and at the first glance it might seem surprising.

There is some evidence to support this hypothesis. Smith *et al* [20] showed that following plasma breakdown there is a net current flowing in the system, which charges the blocking capacitor and forms the self-bias. During the period where the capacitor is charging, the plasma potential is very large, the self-bias voltage on the S-antenna becomes larger and the average plasma potential decreases until the system approaches steady state and no current is flowing in the system [20]. For a grounded antenna, the blocking capacitor no longer exists and the current flowing in the system following the breakdown will continue to go from the plasma through the antenna to

ground. The plasma potential will remain large as electrons are continuously lost to the antenna and the plasma adjusts by losing positive charge as quickly as possible.

We can estimate the plasma loss  $P_{S\text{-antenna}}$  due to ionization, excitation and the kinetic energy carried by electrons and ions to the S-antenna, using the following equation [14];

$$P_{S\text{-antenna}} = 0.6n_i A C_s e (V_i + V_{ex} + 2T_e + V_p - V_{sb}), \quad (6)$$

where  $0.6n_i$  is the sheath edge density [2],  $A = 40 \text{ cm}^2$  is the area of the S-antenna,  $C_s = \sqrt{kT_e/m_i}$  is the ion acoustic velocity where  $k$  is the Boltzmann constant and  $m_i$  is the argon ion mass. The ionization energy  $V_i$  is 15 eV, the excitation energy  $V_{ex}$  is about 13 eV and each electron takes  $2T_e$  with it as it leaves. To this we must add the negative bias voltage  $|V_{sb}|$  on the S-antenna (in the floating case), which generally dominates over all the other terms. The  $P_{S\text{-antenna}}$  calculated for the grounded and floating cases as a function of the S-power is shown in figure 7. The range for power efficiency ( $P_{S\text{-antenna}}/P_{S\text{-power}}$ ) is 40–80% for the floating case and 20–40% for the grounded case, possibly as a result of the expected dc current flowing from the plasma to ground, which lowers the plasma density in the latter case. Suzuki *et al* [21] investigated the power efficiency of an external and internal one loop rf antenna and showed that the power efficiency depends on the plasma density. The power efficiency calculated in the floating case as a function of the measured plasma density shows a trend similar to that of the internal antenna, and suggests that the power transfer changes from a capacitively dominant to an inductively dominant power coupling at about 30 W. The power transfer efficiency in the grounded case is low and indicates that the power coupling is capacitive for the whole power range. The similarity between our ‘magnetized’ plasma, with a differently shaped immersed antenna, to their unmagnetized plasma results suggests that there is similar underlying physics occurring, at least on the general scale of description we are presenting here.

The increase in electron temperature seen in figures 3(c) and 4(c) as the S-power is increased (up to 60 W) is probably due to transit time heating effects close to the antenna (stochastic heating). It has been recently shown [14] that a theoretical estimate of the stochastic heating a few times smaller than an experimental estimate was found in a helicon source. Additional power deposition terms related to capacitive and/or inductive rf currents flowing in the plasma bulk and generated by the S-antenna and/or the H-antenna may

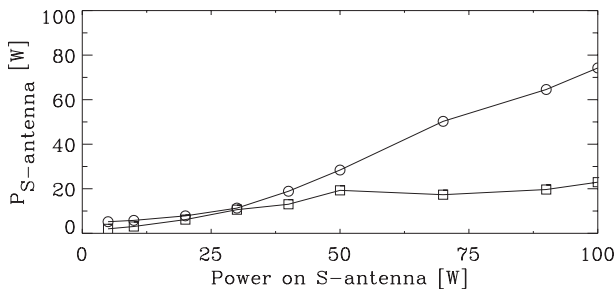


**Figure 7.**  $P_{S\text{-antenna}}$  calculated from equation (5) as a function of the input power on the S-antenna for the grounded ( $\square$ ) and floating ( $\circ$ ) cases.

be present [2, 22]. At a pressure of 4 mTorr, this effect would be limited to the environs of the S-antenna.

When the immersed S-antenna was grounded, many small pinpoint discharges and arcing could be seen in the diffusion chamber at the higher powers ( $\geq 30 \text{ W}$ ), probably due to the large  $V_p$ , and unfortunately resulted in the breakage of the glass source tube. Therefore, the following experiments were performed with the antenna floating, but similar results were seen in the grounded case.

### 3.3. Phase shift effects

Measurements of the plasma parameters as a function of the phase shift between the H- and S-antennae were obtained with the S-antenna floating. The S-antenna was tuned for each phase change while tuning of the H-antenna was unnecessary as its standing wave ratio (SWR) was always close to 1. Figure 8 shows  $V_p$ ,  $V_f$  and  $T_e$  and figure 9 shows  $n_i$ ,  $V_{sb}$  and  $I_{pp}$  as a function of the phase difference between the H- and S-antenna. The H- and S-powers were 150 W and 100 W, respectively. For the phase shift of  $0^\circ$ , a decrease of both  $n_i$  and  $V_{sb}$  by a factor of about 3 is measured compared to the values shown in figure 6 at 100 W S-power. As detailed in a previous publication [13], some sputtering of the copper antenna occurs for 100 W on the S-antenna, which induces a copper coating on the source tube and a power transfer decrease from the H-antenna to the plasma. Consequently, starting with a clean tube, a density

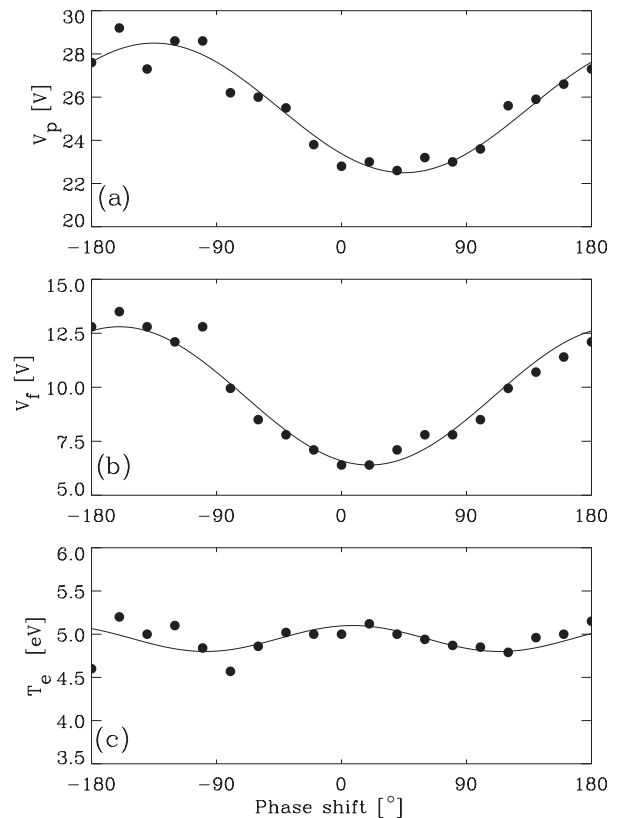


**Figure 8.** (a) Plasma potential  $V_p$ , (b) floating potential  $V_f$ , and (c) electron temperature  $T_e$ , as a function of the phase shift between the H-antenna and the immersed S-antenna. The H-power is 150 W, S-power is 100 W, argon pressure is 4 mTorr and the S-antenna is floating.

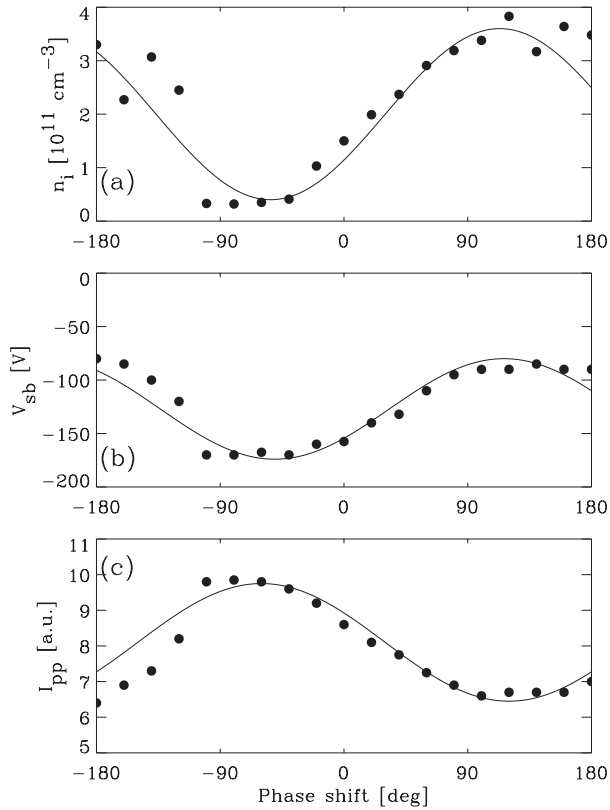


**Figure 9.** (a) Plasma density  $n_i$ , (b) self-bias  $V_{sb}$ , and (c) rf current  $I_{pp}$  as a function of the phase shift between the H-antenna and the immersed S-antenna, for the same conditions as in figure 8.

decrease of a factor of about 3 is measured during the first 30 min of operation. Subsequently, the density remains stable versus time. To prevent any undesirable density drift due to copper re-deposition, the phase shift series was performed in a continuous run over a period of 10 min following the initial density decrease.

Figures 8 and 9 show that there are harmonic sinusoidal like variations with phase-shift between the antennae, where  $n_i$  and  $V_{sb}$  change in phase and  $I_{pp}$  changes in anti-phase ( $180^\circ$ ).  $V_p$  and  $V_f$  are  $90 \pm 15^\circ$  out of phase with respect to  $n_i$ .  $T_e$  seems to change sinusoidally as well, but the amplitude is very small and the frequency is doubled compared to how the other parameters change. The most dramatic variations are evident in the plasma density changing by 80%, and the self-bias and floating potential changing by 40%, while  $I_{pp}$ ,  $V_p$  and  $T_e$  change by 10–20%. Note that these are local measurements close to the immersed antenna (1 cm). However, at 25 cm downstream from the antenna, in the diffusion chamber, the ion saturation current and the floating potential were measured as a function of the phase shift and the sinusoidal like variation was still noticeable. The abrupt change at the phase between  $-80^\circ$  and  $-90^\circ$ , evident in all measured parameters and most pronounced in the plasma density measurements, might be due to a capacitive-to-inductive or inductive-to-helicon mode transition for either the S- or H-antenna.

As the density decreases, the self-bias increases, as would be expected since the power to the S-antenna is kept constant. However, the plasma loss to the S-antenna,  $P_{S\text{-antenna}}$ , as a function of phase is calculated using equation (5) with the

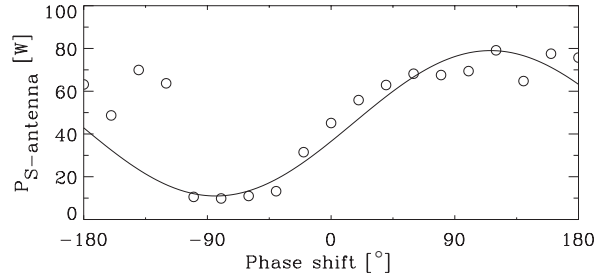


**Figure 10.**  $P_{S\text{-antenna}}$  calculated from equation (5) as a function of the phase shift between the H-antenna and the immersed S-antenna, for the same conditions as in figure 8.

results from figures 8 and 9, and is shown in figure 10. Even though the S-power is kept constant, a periodic sinusoidal like variation is found and is in phase ( $\pm 10^\circ$ ) with the plasma density and self-bias. The maximum calculated power of 80 W agrees well with the power input to the immersed S-antenna of about 100 W (measured at the rf generator), but the minimum calculated power is only about 10 W. A calibration of the rf generator with a high impedance HF-probe was also carried out, and for 100 W at the generator the HF-probe measured 172 V peak-to-peak over  $50 \Omega$ , giving  $P = V_{pp}^2/8R = 74$  W, and for 20 W we measured 87 V which corresponds to 19 W. The plasma loss,  $P_{S\text{-antenna}}$ , is similar to the power input, S-power, for most values of the phase, except for phases between  $-110^\circ$  and  $-30^\circ$ . In that phase range the calculated power is about 10 W and it remains unclear where the rest of the power goes. A rf power loss of many tens of watts may occur in the matching box/antenna (eddy and skin currents and antenna radiation) as observed by many authors [14, 21]. This result also agrees with a maximum measured current  $I_{pp}$  circulating in the S-antenna/matching box for phases between  $-110^\circ$  and  $-30^\circ$  (figure 9(c)).

Thomas and Singh [7] also report on sinusoidal variation in the electrode voltages (rf peak to peak) and self-bias as a function of phase between the electrodes in a balanced triode plasma etching reactor. The phase between two electrodes in rf sputtering systems have also been shown to influence both particle concentration, ion energy distribution, and self-bias potentials previously [9, 10, 23]. Although the influence of the phase between rf antennae/substrates has been known and reported on previously, the effect on the plasma parameters are still not very well understood. Interference and dephasing between the two rf sources might occur, and it has been shown theoretically that two rf sources can nonlinearly interact if the frequencies are sufficiently close. The resulting plasma and electrical characteristics can then be significantly different [6]. The variation of the floating and plasma potentials is  $90^\circ$  out of phase with the self-bias and with the density. This behaviour suggests that the system is acting as a forced oscillator and may be open to theoretical interpretation. The changes in density with phase are probably due to changes in the phase difference between the rf on the plasma potential and that of the S-antenna. For angles around  $-90^\circ$  the oscillations in the plasma potential generated by the helicon antenna (which are not small [12]) might serve to decrease the electron heating effect of the S-antenna fields. For phase angles around  $+90^\circ$ , the two potential variations would appear to be in phase and thus add to the heating efficiency of the S-antenna [22].

The substrate rf power including the matching network losses has been modelled (empirically) as a function of the 'delay cable length' between the substrate and cathode in an rf sputtering system [8]. The 'delay cable length' corresponds to the phase delay between the substrate and the cathode, and the calculation showed a sinusoidal variation similar to the one in figure 10. The authors also find that the cable length affects the ion and electron energies, the peak-to-peak voltage on both the substrate and cathode and the rf plasma voltage, and all parameters have a sinusoidal variation in agreement with the results presented here. It is possible that a modification of the rf equivalent circuit model proposed by Logan *et al* [8] could be used to predict the phase-shift dependence on the plasma parameters in our system as well, by the use of two oscillators. This will be the subject of further work.

#### 4. Conclusion

For a magnetic field of 100 G presented here, the effect of the immersed antenna is felt all over the plasma and not only on the field lines which intersect it. This is different to magnetic fields of kilo-Gauss where the electron heating seems more localized and confined to magnetic field lines connected to the antenna. We believe that the phenomenon described in this paper may also be present in the H1 Heliac.

The behaviour of an antenna immersed in, and in contact with, a plasma is very different when it is electrically floating and when it is grounded. In the former case, a self-bias forms on the antenna and the floating and plasma potentials change little with increasing power. In the latter case, the plasma charges up and a dc current can flow from the plasma to the antenna to ground. It is shown that the plasma potential in the grounded case is equal to the sum of the plasma potential and self-bias in the floating case. Hence, the sheath generated between the S-antenna and the plasma is equal in both cases. In the floating case, as long as the S-power is low, and not affecting the bulk plasma, the self-bias increases linearly with S-power, while at larger powers when the power is coupled inductively to the plasma the self-bias is fairly constant.

As the phase shift between the 13.56 MHz helicon antenna and the immersed copper antenna (with the same frequency) is varied, the plasma parameters change dramatically: the plasma density, plasma and floating potential, self-bias and rf-current are all observed to change markedly, and can be fitted to a sinusoidal function. The variation of the measured parameters was internally consistent, and showed that the calculated power to the immersed antenna changed in a similar manner to the self-bias and the plasma density and inversely to the rf-current. The calculated maximum power on the S-antenna was in quite good agreement with the actual power from the generator.

#### Acknowledgments

This work has been carried out in the Plasma Research Laboratory, at the Australian National University. The authors are grateful for the technical assistance of Peter Alexander. Ane Aanesland was supported by the Norwegian Research Council (Grant No 131953/432), and extends her thanks to Rod Boswell and Christine Charles for their friendly hospitality during her stay at ANU.

#### References

- [1] Butler H S and Kino G S 1963 *Phys. Fluids* **6** 1346
- [2] Lieberman M A and Lichtenberg A J 1994 *Principles of Plasma Discharges and Materials Processing* (New York: Wiley)
- [3] Shats M G, Rudakov D L, Boswell R W and Borg G G 1997 *Phys. Plasmas* **4** 3629
- [4] Collins G A and Tendys J 1994 *J. Vac. Sci. Technol. B* **12** 875
- [5] Collins G A, Short K T and Tendys J 1997 *Surf. Coat. Technol.* **93** 181
- [6] Rauf S and Kushner M J 1999 *IEEE Trans. Plasma Sci.* **27** 1329
- [7] Thomas III J H and Singh B 1992 *J. Vac. Sci. Technol. A* **10** 3070
- [8] Logan J S, Keller J H and Simmons R G 1977 *J. Vac. Sci. Technol.* **14** 92
- [9] Kamata T and Arimoto H 1996 *J. Vac. Sci. Technol. B* **14** 3688
- [10] Tsuda O, Tatebayashi Y, Takamura Y Y and Yoshida T 1999 *Plasma Sources Sci. Technol.* **8** 392
- [11] Chi K-K, Sheridan T E and Boswell R W 1999 *Plasma Sources Sci. Technol.* **8** 421
- [12] Charles C, Degeling A W, Sheridan T E, Harris J H, Lieberman M A and Boswell R W 2000 *Phys. Plasmas* **7** 5232
- [13] Aanesland A, Charles C, Boswell R W and Fredriksen Å 2003 *Plasma Sources Sci. Technol.* **12** 85
- [14] Charles C, Boswell R W and Lieberman M A 2003 *Phys. Plasmas* **10** 891
- [15] Hutchinson I H 1987 *Principles of Plasma Diagnostics* (Cambridge: Cambridge University Press)
- [16] Flender U, Nguyen Thi B H, Wiesemann K, Khromov N A and Kolokolov N B 1996 *Plasma Sources Sci. Technol.* **5** 61
- [17] Aanesland A and Fredriksen Å 2001 *J. Vac. Sci. Technol. A* **19** 2446
- [18] Goto H H, Lowe H-D and Ohmi T 1993 *IEEE Trans. Semicond. Manu.* **6** 58
- [19] Kim H C and Manousiouthakis V I 1998 *J. Vac. Sci. Technol. A* **16** 2162
- [20] Smith H B, Charles C, Boswell R W and Kuwahara H 1997 *J. Appl. Phys.* **82** 561
- [21] Suzuki K, Nakamura K, Ohkubo H and Sugai H 1998 *Plasma Sources Sci. Technol.* **7** 13
- [22] Lieberman M A and Godyak V A 1998 *IEEE Trans. Plasma Sci.* **26** 955
- [23] Tsuda O, Yamada Y, Fujii T and Yoshida T 1995 *J. Vac. Sci. Technol. A* **13** 2843